# Preparation of Amino-Functionalized Graphene Sheets and their Conductive Properties

A.A. Arbuzov[1,*], V.E. Muradyan[1,†], B.P. Tarasov[1], E.A. Sokolov[2]

[1] *Institute of Problem of Chemical Physics RAS, 1, Acad. Semenov's, 142432 Chernogolovka, Russia*
[2] *Institute of Energy Problems for Chemical Physics (branch), 1, Acad. Semenov's, 142432 Chernogolovka, Russia*

Amino-functionalized graphene sheets were prepared through chemical reduction by hydrazine hydrate, amination or amidation of graphite oxide. For amination of graphite oxide were used polyamine such as ethylenediamine, diethylenetriamine and triethylenetetramine. Addition of amine groups to graphene is identified by Fourier transform infrared spectroscopy, Raman spectroscopy, elemental analysis and thermogravimetry. Scanning electron microscopy data indicate that the organic amine is not only as nitrogen sources to obtain the nitrogen-doped graphene but also as an important modification to control the assembly of graphene sheets in the 3D structures. The electrical conductivity of the materials obtained by amination and amidation of graphene is much smaller than that of reduced graphite oxide.

**Keywords:** Graphite Oxide, Amino-Functionalized Graphene, Electrical Conductivity.

PACS numbers: 81.05.Ue, 81.40.Rs

## 1. INTRODUCTION

Graphene sheets are planar monolayers of $sp^2$-bonded carbon atoms tightly packed into a two-dimensional honeycomb lattice [1]. Graphene has extraordinary electronic [2], thermal [3] and mechanical [4] properties. Moreover, after functionalization, graphene is expected to serve as nanofiller in composite materials. Comparing with carbon nanotubes (**CNTs**), graphene can offer better thermal, mechanical, and electrical properties [5]. Owing to these fundamental properties, graphene has attracted a great interest for many potential applications nowadays, such as nanoelectronics, and molecular devices.

The application of graphene as nanofiller relies critically on the homogeneous dispersion of graphene throughout the matrix. Due to the special two dimensional structures, high surface energy, and intrinsic van der Waals forces, graphene is apt to aggregate and entangle together spontaneously. This hinders the uniform distribution of graphene in the polymer matrix and thus reduces the effect of graphene.

These problems are overcome by the functionalization of graphene, which can provide multiple bonding sites to the resin matrix so that the unique properties of graphene can be successfully transferred to polymer composite. Amine group displays high reactivity and contains a wealth of chemistry, which enables it to react with many other chemicals easily. Former studies about the amino-functionalized CNTs show that different amino groups on surface of the CNTs have a great effect on their dispersibility in different solvents. Compared with the native polymer and the unmodified CNT-based polymer composites, the properties of amino-functionalized CNT-reinforced polymer matrices show great improvement [6-8]. The addition of graphene into a polymer matrix allows the creation of composite materials with improved properties such as reinforcement, electrical conductivity, electromagnetic absorption and other.

Graphite oxide (**GO**) is a layered material produced by the oxidation of graphite. Currently, GO is prepared mostly based on the method proposed by Hummers and Offeman [9] in 1958, where the oxidation of graphite to graphite oxide is accomplished by treating graphite with a water-free mixture of concentrated sulfuric acid, sodium nitrate and potassium permanganate. In contrast to pristine graphite, the graphene sheets in graphite oxide are heavily oxygenated, bearing hydroxyl and epoxide functional groups on their basal planes, in addition to carbonyl and carboxyl groups located at the sheet edges. The presence of these chemical groups makes the amino-functionalization of graphene sheets much easier.

In this work, amino-functionalized graphene sheets were obtained by three methods: 1) chemical reduction of GO by hydrazine; 2) acylation of GO, followed by amidation octadecylamine (**ODA**); 3) amination of GO. For amination of GO were used ethylenediamine (**E**), diethylenetriamine (**D**) and triethylenetetramine (**T**).

## 2. EXPERIMENTAL

### 2.1 Synthesis of GO

GO was prepared using a modified Hummers and Offeman's method from natural graphite [10]. In brief, 25 g of the natural graphite powder and 12.5 g of $NaNO_3$ was added into a 2 L three-necked flask and 700 mL of $H_2SO_4$ were added subsequently under stirring in an ice-bath. After obtaining blue colored graphite bisulfate 82.5 g of $KMnO_4$ was added slowly into the flask under stirring condition and the temperature of the mixture was controlled up to 20 °C. After 5 min the ice-bath was removed and the mixture allowed to warm no greater than 50 °C. The mixture was kept at ambient temperature for about 8 h. Then 1 L water was slowly added into the mixture and stirring was continued for another 1 h. The mixture was

poured into a 2 liter beaker and slowly added drop-wise 3% $H_2O_2$ aqueous solution were added to reduce the residual $KMnO_4$ until the reed yellow color of graphite oxide. Finally, mixture was washed bidistilled water by decantation until sulphate ions could not be detected with $BaCl_2$.

## 2.2 Reduction of GO

To 40 g aqueous suspension of GO (1 wt.%) was added 150 mL of $H_2O$ and 2 mL of ammonia solution, the resulting mixture was treated on a ultrasonic bath. To the mixture was added 2 mL of hydrazine hydrate and refluxed for 8 h. The resulting precipitate was filtered on a glass filter and washed extensively with bidistilled water until pH ~7. The resultant reduction graphite oxide (**RGO**) was dried under vacuum at 80 °C.

## 2.3 Amination of GO (AmGOs)

0.5 g of dried graphite oxide was ultrasonicated in 50 mL of 1-butanol to obtain a uniform dispersion. Then 10 mL of amine (E, D, and T) was added to mixture and refluxed for 8 h. Afterwards, the solid were separated by filtration and washed with excess ethanol and dried under vacuum at 80 °C.

## 2.4 Amidation of GO (AdGO)

For the amidation to 0.5 g of dried graphite oxide was added 50 mL of thionyl chloride ($SOCl_2$), 0.5 mL dimethylformamide and refluxed for 24 h. To the resulting mixture was added 50 ml of toluene and excess $SOCl_2$ was distilled off in a stream of argon, together with a portion of toluene. Acyl-chlorinated GO were refluxed with 1 g of ODA for 7 days. After cooling to room temperature, the AdGO were separated by filtration and washed with ethanol and acetone to remove excess amine. Finally, the solid of AdGO was dried under vacuum at 80 °C

## 2.5 Material characterization

All the samples were characterized by Fourier transform infrared spectroscopy (FTIR) using a Perkin-Elmer Spectrum 100 FTIR spectrometer (0.5 $cm^{-1}$ resolution). Raman spectra were measured using a Horiba Jobin Yvon T64000 Raman spectrometer with an argon laser of 514.5 nm. C, H, N and O content analysis of the samples were carried out using a «Vario Micro cube» Elementar GmbH CHNS/O analyzer. The thermal properties of the samples were characterized by thermogravimetry (TGA) using Simultaneous Thermogravimetry Analyzer NETZSCH STA 409 C Luxx, and all the measurements were carried out under argon gas over a temperature range of 30–1000 °C with a ramp rate of 10 °C $min^{-1}$. Scanning electron microscopy (SEM) images were obtained using a scanning electron microscope Zeiss LEO SUPRA 25.

To measure the conductivity of the samples were placed in a plexiglass cylinder with a diameter of 12.6 mm, the bottom of which was an electrode. Using a weight 5.5 kg with an attached electrode powder was pressed to form a tablet with a height of about 5-6

mm. Electrical resistance of tablets was measured universal voltmeter with resistance measurement range of $10^{-2}$–$10^{-7}$ Ohms. The data represent an average of three measurements, the results of which differ not more than 3%, indicating good reproducibility.

## 3. RESULTS AND DISCUSSION

FTIR was applied to monitor the transformation from GO to RGO, AmGOs and AdGO. Many oxygen-containing functional groups are detected in GO (Fig. 1, curve 1). A broad absorption peaks at ~3420 $cm^{-1}$ which is related to the O–H stretching vibrations in the water and hydroxyl groups in the GO; the C=O stretching vibrations in the carboxyl group at 1733 $cm^{-1}$; the C=C ring stretching at 1624 $cm^{-1}$; the O–H deformation from the hydroxyl groups attached to the aromatic graphene network at 1407 $cm^{-1}$; the C–O (hydroxy) stretching at 1068 $cm^{-1}$; the C–O (epoxy) stretching at 982 $cm^{-1}$; and the C–H stretching at 1228 $cm^{-1}$. In the FTIR spectrum of RGO (curve 5) the intensity of the peaks for oxygen functional groups (~3420, 1733, 1407, 1068 and 1228 $cm^{-1}$) disappears completely. However the absorption peaks related to skeletal vibration of the aromatic rings were observed in the RGO but the peak position shifted from 1624 to 1655 $cm^{-1}$ with respect to GO. A new absorption band that appears at 1560 $cm^{-1}$ may be attributed to the N–H in-plane stretching.
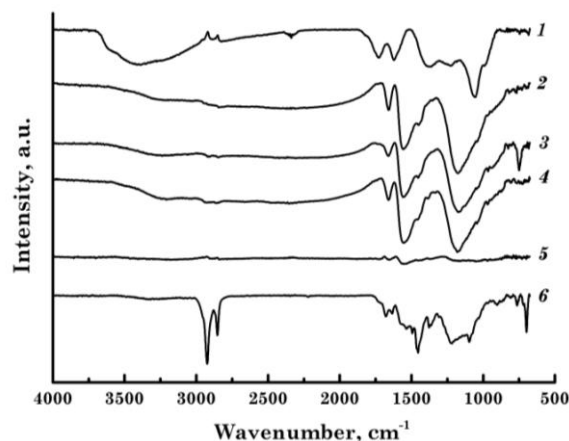


**Fig. 1** – FTIR spectra for GO (1), AmGO-T (2), AmGO-D (3), AmGO-E (4), RGO (5), and AdGO (6).

In all amino-functionalized GO samples (Fig. 1, curve 2, 3, 4, 6) peaks at about 3400 $cm^{-1}$ were found which can be associated with N–H stretching vibration; the N–H deformation peaks at 1560 $cm^{-1}$ (AmGOs) and 1577 $cm^{-1}$ (AdGO); the C–N stretching vibrations at 1180 $cm^{-1}$ (AmGOs) and 1220 $cm^{-1}$ (AdGO). The C=C stretching vibration of benzene ring of AmGO-T (1658 $cm^{-1}$), AmGO-D (1659 $cm^{-1}$), AmGO-E (1658 $cm^{-1}$) and AdGO (1635 $cm^{-1}$) were also found. Moreover the FTIR spectrum of AdGO has peaks at 2925 and 2853 $cm^{-1}$ which is related to the C–H stretch of alkyl chain; the C=O stretching vibrations in the amide group at 1733 $cm^{-1}$; and the C–O stretching in the hydroxyl groups at 982 $cm^{-1}$. The FTIR spectra provide the evidence of successful introduction of nitrogen and reduction of GO. During amination the amino group can be reacted with carboxylic acid species to form an amide-like structure, which then by decarbonylation

can form stable aromatic and other structures as the imine. Those amines can also react with other oxygen-containing moieties to reduce graphene oxide.

SEM images revealed that the reduced GO material consists of randomly aggregated, thin, crumpled sheets closely associated with each other and forming a disordered solid (Fig. 2b). The folded regions of the sheets were found to have average widths of ~2 nm.
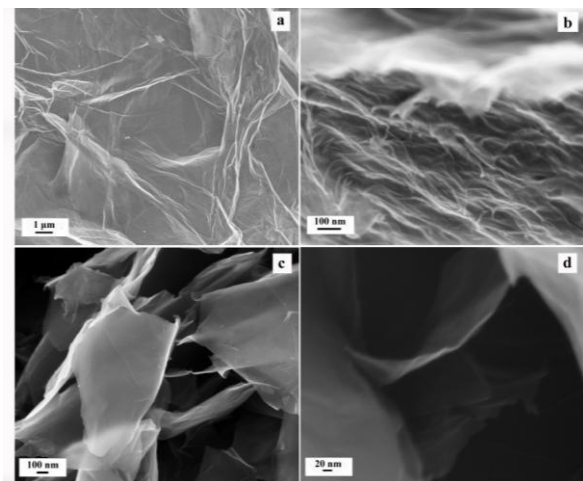


**Fig. 2** – SEM images of GO (a), RGO (b), and AmGO-E (c), (d)

Attaching amine to the carbon plane strongly influences on the structure of AmGOs and AdGO (Fig. 2b and 2c). It can expand space between graphene sheets because of the tail chain of the organic amine outside the plane and form new hydrogen bonds. In addition, it can hinder the $\pi$–$\pi$ stacking in single graphene sheet. Therefore, the bigger porous network and much flatter graphene structure compared with the RGO can be obtained.

The elemental analysis data (carbon, hydrogen, nitrogen and oxygen) of GO, RGO, AmGOs and AdGO were summarized in Table 1.

**Table 1** – Compositions of GO, RGO, AmGOs and AdGO.

|  | Elemental analysis, wt.% | | | |
|---|---|---|---|---|
|  | C | H | N | O |
| GO | 49.3 | 2.4 | 0.0 | 45.1 |
| RGO | 87.8 | 0.6 | 3.3 | 8.3 |
| AmGO-E | 75.8 | 2.7 | 13.9 | 7.6 |
| AmGO-D | 82.0 | 3.6 | 10.0 | 4.4 |
| AmGO-T | 69.3 | 3.9 | 14.4 | 12.4 |
| AdGO | 76.9 | 5.7 | 2.2 | 13.1 |

The atomic ratio of C/O for RGO, AmGO-E AmGO-D, AmGO-T and AdGO is about 14.1, 13.2, 24.8, 7.5 and 5.9, respectively. It is much higher than that of GO (2.7), which indicates the de-oxygenation of GO during the reaction. The C, H, N and O element analyses of the samples lead to the following nominal compositions for the amine-functionalized samples, which confirmed the amino-functionalization. Thus RGO has the nominal formula – $C_{100}H_{8.2}N_{3.3}O_{7.1}$; E-functionalized – $C_{10.6}O_{0.9}(E)$; D-functionalized – $C_{24.9}H_{4.2}O_{1.2}(D)$; T-functionalized – $C_{16.7}O_{3.1}(T)$; ODA-functionalized – $C_{22.2}O_{5.2}(ODA)$.

TGA is a complementary technique that can reveal the composition and the thermal stability. Figure 3

shows the thermogravimetric profiles of GO, AmGOs and AdGO. Although GO is thermally unstable and starts to lose mass upon heating even below 100 °C, the major mass loss occurs at about 110 °C, presumably due to pyrolysis of the labile oxygen-containing functional groups, yielding CO, $CO_2$, and steam (Fig. 3, curve 5).
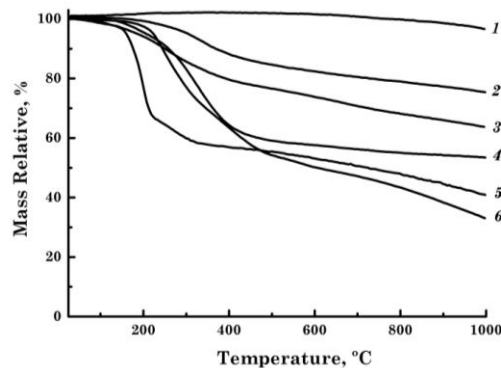


**Fig. 3** – TGA analysis of RGO (1), AmGO-D (2), AmGO-E (3), AmGO-T (4), GO (5), and AdGO (6)

On the other hand, the removal of the thermally labile oxygen-containing functional groups by chemical reduction results in much increased thermal stability for the RGO (Fig. 3, curve 1). Apart from a slight mass loss below 100 °C, which can be attributed to the loss of adsorbed water, no significant mass loss is detected when this material is heated up to 1000 °C. Compared with GO, the thermal stability of AmGOs and AdGO Fig. 3, curve 2–6) increased after the amino-functionalization. Along with the amino functionalization observed a loss of oxygen-containing functional groups and the resulting thermal stability of AmGOs and AdGO higher than that of GO. The decomposition temperature of AmGO-E, AmGO-D, AmGO-T and AdGO is 130, 170, 135 and 165 °C, respectively.
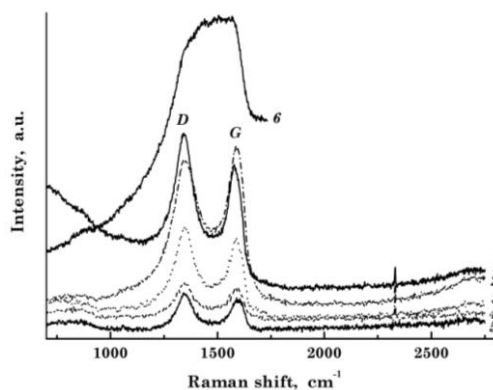


**Fig. 4** – Raman spectra of GO (1), AmGO-D (2), AmGO-E (3), AmGO-T (4), RGO (5) and AdGO (6)

The changes of structure from GO to RGO, AmGOs and AdGO by chemical reduction and amino-functionalization are also reflected in the Raman spectroscopy. The Raman spectrum of the pristine graphite displays a prominent *G* band with $E_{2g}$ symmetry at 1580 cm$^{-1}$, is related to phonon vibrations in $sp^2$ carbon materials [11]. In the Raman spectrum of GO (Fig. 4, curve 1), the *G* band is broadened and shifted to

1590 cm$^{-1}$. In addition there is a *D* band with A$_{1g}$ symmetry at 1354 cm$^{-1}$, indicating the destruction of *sp$^2$* character and the formation of defects in the sheets due to extensive oxidation.

The Raman spectrum of the RGO (Fig. 4, curve 5) also contains both *G* and *D* bands (at 1595 and 1349 cm$^{-1}$, respectively); however, with an increased *D*/*G* intensity ratio (1.26) compared with GO (0.96). The Raman spectrum of AmGOs also displays *D* band and *G* band, *D*/*G* intensity ratio of AmGO-E, AmGO-D and AmGO-T is 1.15, 1.15 and 1.13, respectively. Moreover, compared with the RGO the *G* band of the AmGO-E, AmGO-D and AmGO-T is down-shifted to 1585, 1578 and 1583 cm$^{-1}$, respectively. The downshift of the *G* band can be attributed to electron-donating capability of nitrogen heteroatoms.

Electrical conductivity of RGO is 41.7 S/m, which is significantly less than the natural graphite (330 S/m) measured by the same method. It can be related to formation of defects in the oxidation of graphite which do not heal under chemical reduction. These defects prevent the electron transport thereby reducing electrical conductivity. AmGO-D, AmGO-E , AmGO-T and AdGO exhibit lower conductivity values than RGO is 1.4, 6.7×10$^{-1}$, 3.7×10$^{-1}$ and 2.3×10$^{-2}$ S/m, respectively. This can be explained by the fact that the amino functionalization produce large amounts of *sp$^3$* hybridized carbon atoms due to the formation of C–N bond. Thus the decrease in the conductivity due to destruction of delocalized π-system.

## 4. CONCLUSION

In recent years, studies on chemical modification of graphene have attracted tremendous attention. In our study three types of amino-functionalized graphene sheet were prepared through chemical reduction by hydrazine hydrate, amination and amidation of GO. The experimental results provide evidence that the interaction of GO with amines such as ethylenediamine, diethylenetriamine and triethylenetetramine along with the addition of an amine group also leads to a partial reduction. It is shown that the introduced amine in the carbon plane strongly influences on the structure and electrical conductivity properties.

## REFERENCES

1. K.S. Novoselov, A.K. Geim, S.V. Morozov, D. Jiang, Y. Zhang, S.V. Dubonos, I.V. Grigorieva, A.A. Firsov, *Science* **306**, 666 (2004).
2. M. Orlita, C. Faugeras, P. Plochocka, P. Neugebauer, G. Martinez,D.K. Maude, A.-L. Barra, M. Sprinkle, C. Berger, W.A. de Heer, M. Potemski, *Phys. Rev. Lett.* **101**, 267601 (2008).
3. A.A. Balandin, S. Ghosh, W. Bao, I. Calizo, D. Teweldebrhan, F. Miao, Ch.N. Lau, *Nano Lett.* **8**, 902 (2008).
4. C.G. Lee, X.D. Wei, J.W. Kysar, J. Hone, *Science* **321**, 385 (2008).
5. S. Stankovich, D.A. Dikin, G.H.B. Dommett, K.M. Kohlhaas, E.J. Zimney, E.A. Stach, R.D. Piner, S.T. Nguyen, R.S. Ruoff, *Nature* **442**, 282 (2006).
6. J.F. Shen, W.S. Huang, L.P. Wu, M.X. Ye, *Mater. Sci. Eng. A.* **464**, 151 (2007).
7. S. Frankland, V. Harik, *Surf. Sci.* **525**, 103 (2003).
8. F. Gojny, J. Nastalczyk, Z. Roslaniec, K. Schulte, *Chem. Phys. Lett.* **370**, 820 (2003).
9. W.S. Hummers, R.E. Offeman, *J. Am. Chem. Soc.* **80**, 1339 (1958).
10. V.E. Muradyan, V.S. Romanova, A.P. Moravsky, Z.N. Parnes, Yu.N. Novikov, *Russ. Chem. Bull.* **49**, 1017 (2000).
11. Y. Si, E.T. Samulski, *Nano Lett.* **8**, 1679 (2008).